Improved light coupling efficiency of organic light-emitting diode and polymer optical waveguide integrated device by grating coupler*

WEI Song (魏松), **LIU Chang** (刘畅), **QIN Houyun** (秦后运), **LIU Yiming** (刘一鸣), **CHEN Changming** (陈长鸣), **WANG Hongbo** (王红波), **and ZHAO Yi** (赵毅)**

State Key Laboratory of Integrated Optoelectronics, College of Electronic Science and Engineering, Jilin University, Changchun 130012, China

(Received 28 January 2021; Revised 12 March 2021)

In this work, the light coupling efficiency of organic light-emitting diode (OLED) and polymer optical waveguide integrated device was improved by the grating coupler. To maximize light coupling efficiency, the grating coupler was optimized by finite-difference time-domain (FDTD) method. Based on the simulation results, the grating coupler was fabricated via laser interference lithography process and an OLED was integrated on the surface of it. Comparing the integrated devices without and with grating coupler, light coupling efficiency of the grating-based integrated device was improved by about 5%. The proposed integrated device has the potential application for low-cost and flexible monolithic optical sensors.

Document code: A **Article ID:** 1673-1905(2021)10-0598-6

DOI https://doi.org/10.1007/s11801-021-1011-8

At present, integrated optoelectronic technology based on polymer optical waveguide have been widely applied in short distance optical communication[1,2] and optical sensing[3,4] due to its merits of mechanical flexibility and biocompatibility. Generally, these kinds of integrated optoelectronic applications require external light sources, such as light-emitting diodes or diode-pumped solid-state lasers which are difficult to achieve monolithic integration and flexibility. However, in some specific scenarios of optical sensing application, such as disposable medical diagnostic[3,5] or pressure sensing on the curved surface of robot hand[6], a monolithic integrated optoelectronic device with the features of low-cost, portable and flexible is in great demand. Such kind of monolithic integrated optoelectronic device consists of light sources, polymer optical waveguides and photodetectors to realize sensing function[7]. When optical signals transmitted in optical waveguide interact with biomolecule on the surface of the waveguide or the thickness of waveguide is changed, the wavelength or intensity of the optical signals will be varied and be detected by photodetector[4,8,9]. The optical signals can be provided by light sources which require the features of flexibility and easy integration. Since the organic light-emitting diode (OLED) has great advantages of low cost, flexibility and easy integration with other substrates[10], which could be suitable for directly integrating with the polymer optical waveguide as a monolithic integrated light source. Nevertheless, the light intensity of the OLED is still insufficient compared with inorganic light-emitting device. Meanwhile, the light coupling efficiency between the OLED and polymer optical waveguide is limited by the low refractive index contrast between the waveguide core and cladding[11]. Ohmori et al[12] used a 45° Au coated cut mirror to introduce the output light from the OLED reflect to the waveguide core. Although this approach realized the integration of an OLED and polymer optical waveguide, the preparation process of the 45° Au cut mirror is complex. Lin et al[13] used the SiO_2 diffuser particles dispersed in SU-8 waveguide to enhance the scattering of the light from a polymer light-emitting diode (PLED) into the SU-8 waveguide, but the light coupling efficiency was only 1%. Therefore, the further enhancement of the light coupling efficiency to increase the sensitivity of the integrated device is a challenge task[14].

In this paper, we improved the light coupling efficiency of an OLED and polymer optical waveguide integrated device by employing an embossed grating coupler. Furthermore, an MoO_x buffer layer was designed for the deposition of the OLED. Such kind of grating coupler with an MoO_x buffer layer could not only improve the light coupling efficiency but also maintain the electrical properties of the integrated OLED without degradation. In order to enhance light coupling efficiency, the grating-based integrated device of an OLED and polymer optical waveguide was simulated by FDTD method. Bas-

* This work has been supported by the National Natural Science Foundation of China (No.61675089).

** E-mail: yizhao@jlu.edu.cn

ed on the simulation results, an OLED was deposited on the surface of the grating coupler with an MoO_x buffer layer. Compared the integrated devices without and with grating coupler, the light coupling efficiency of the grating-based integrated device was improved about 5%. The proposed integrated device holds the promise for low-cost and flexible monolithic optical sensors.

To maximize the light coupling efficiency, we designed the integrated device of an OLED and polymer optical waveguide based on grating coupler and optimized the grating coupler by numerical method[15]. Fig.1(a) shows the schematic of an OLED and SU-8 waveguide integrated device based on grating coupler. The photoresist of SU-8 is used as the waveguide core, which has high visible light transmittance and low loss[16,17]. The grating coupler can diffract the optical wave and spread out in all directions and a part of the light will be coupled into SU-8 due to the total internal reflection. The grating parameters which include grating period Λ, etch depth d and duty cycle f.

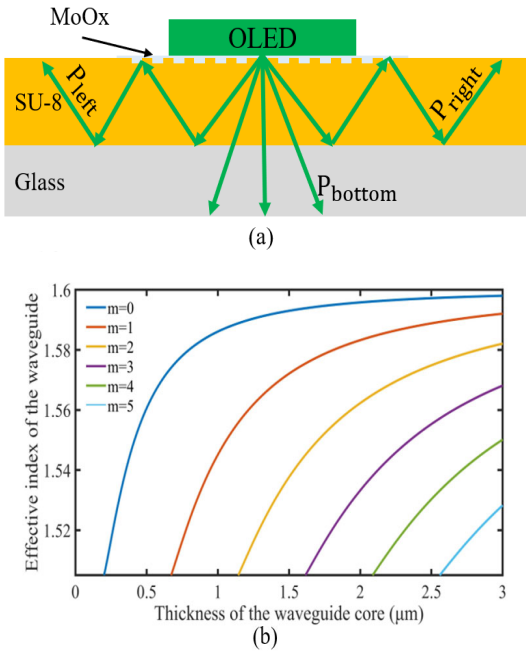

Fig.1 (a) The schematic of an OLED and SU-8 polymer optical waveguide integrated device based on grating coupler; (b) The effective refractive index of TE guided mode as a function of the waveguide core thickness *h*

Normally, the light is coupled into the waveguide through the grating coupler which grating period needs meet the Bragg condition[18,19]

$$\Lambda = \frac{q\lambda}{N_{\text{eff}} \pm n_{\text{c}} \sin\phi}, \tag{1}$$

where λ, q, n_{c}, ϕ and N_{eff} are the wavelength of the incident light, the diffractive order of the grating, the refractive index of the cladding, the incident angle of the light and the effective refractive index of the guided mode, respectively. Here the wavelength of λ=520 nm is the central wavelength of the integrated OLED and the incident angle ϕ of the light is 0° for the case of vertical coupling[20]. For the first order (q=1) of the grating coupling, Λ can be expressed as

$$\Lambda = \frac{\lambda}{N_{\text{eff}}}. \tag{2}$$

where N_{eff} can be obtained from the mode equation of planar waveguide for TE mode[21] by the following equation

$$\left(n_2^2 - N_{\text{eff}}^2\right)^{\frac{1}{2}} \cdot \frac{2\pi}{\lambda} \cdot h = m\pi + \arctan\left(\frac{N_{\text{eff}}^2 - n_1^2}{n_2^2 - N_{\text{eff}}^2}\right)^{\frac{1}{2}} + \arctan\left(\frac{N_{\text{eff}}^2 - n_3^2}{n_2^2 - N_{\text{eff}}^2}\right)^{\frac{1}{2}}, \tag{3}$$

where m and h are the order of the guided mode and the thickness of SU-8 waveguide core, respectively. The refractive index of air cladding, SU-8 waveguide and glass substrate are n_1=1, n_2=1.6 and n_3=1.5, respectively. Fig.1(b) shows the effective refractive index of TE guided mode as a function of the waveguide core thickness h according to Eq.(3). In our work, the thickness of the SU-8 waveguide was chosen to be 2 μm, which was a multimode waveguide. Hence for TE mode, N_{eff} was 1.533 for the third-order (m=3) guided mode as shown in Fig.1(b). Then Λ was calculated to 339 nm by Eq.(2), which was a reference value for the further optimization. Besides, the grating depth d was set to 15 nm and the duty cycle f was fixed to 0.5.

Since the etch depth of the grating affects the flatness of the waveguide surface, a 20-nm-thick MoO_x buffer layer which has high visible light transmittance[22] was designed before the deposition of the OLED. Based on these structure parameters, Λ was further optimized by FDTD simulation[23,24]. Fig.2(a) shows the refractive index distribution of the simulation model with the simplified OLED structure of Ag (18 nm)/Al (2 nm)/Organic (95 nm)/Al (100 nm). The refractive indices of the organic layer and MoO_x layer are 1.75 and 2.1 at λ=520 nm, which were measured by spectroscopic ellipsometer. The radiating molecule in the OLED emitting layer was modeled as a dipole[25]. Perfectly matched layers boundary condition was employed to avoid the parasitic reflection[19]. Here, the light coupling efficiency η can be defined by

$$\eta = \frac{P_{\text{right}} + P_{\text{left}}}{P_{\text{bottom}} + P_{\text{right}} + P_{\text{left}}}, \tag{4}$$

where P_{right} and P_{left} are the optical power of the right and left light coupled into the SU-8 waveguide, and P_{bottom} is the optical power of light transmitted into the glass substrate, as shown in Fig.1(a). Without the grating coupler, the coupling efficiency was only 4.25% by simulations. After employing a grating coupler, the coupling efficiency was raised to 10.9% at Λ=310 nm as shown in

Fig.2(b), which indicated that the coupling efficiency was improved 6.65%. To investigate the effect of the grating coupler, the local electric field intensity distribution of the simulation model with Λ=310 nm and without grating are shown in Figs.2(c) and (d). Comparing Fig.2(c) with Fig.2(d), the direction of electric field became more divergent due to the grating coupler, which helped to enhance the mode coupling of the light into waveguide core. Meanwhile, Fig.2(e) shows the four guided modes transmitting in the SU-8 waveguide, which was consistent with previous designs.

Based on the aforementioned simulation results, we used a two-step exposure method[26] to fabricate the waveguide grating coupler and an OLED was deposited on the surface of the grating coupler with an MoO_x buffer layer. Fig.3(a) shows the fabrication procedure of an OLED and SU-8 waveguide integrated device based on grating coupler. The ~2-μm-thick photoresist of SU-8

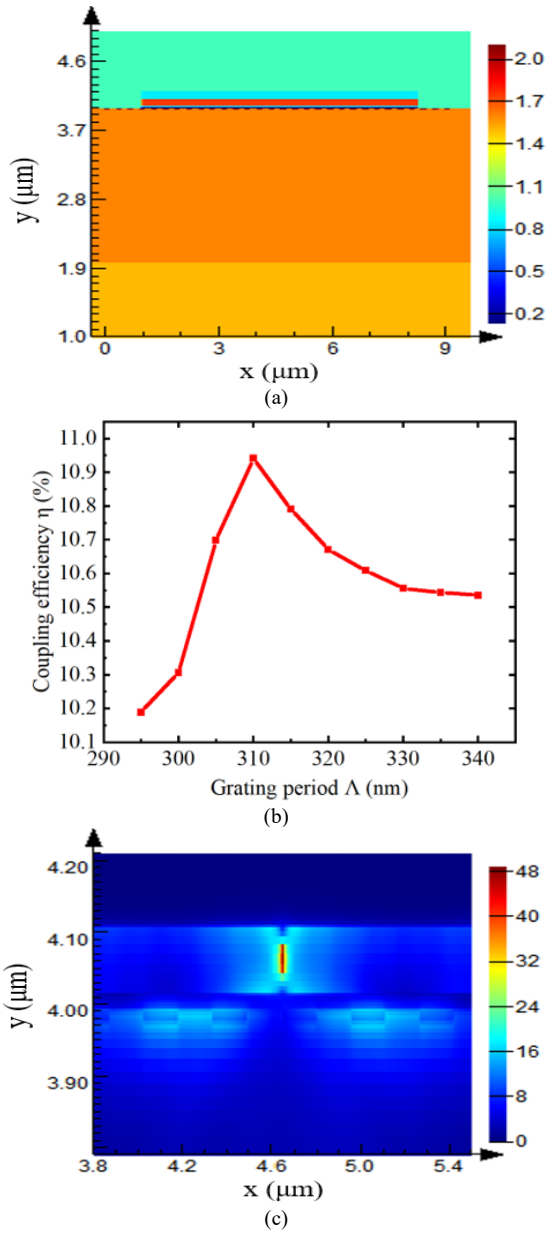

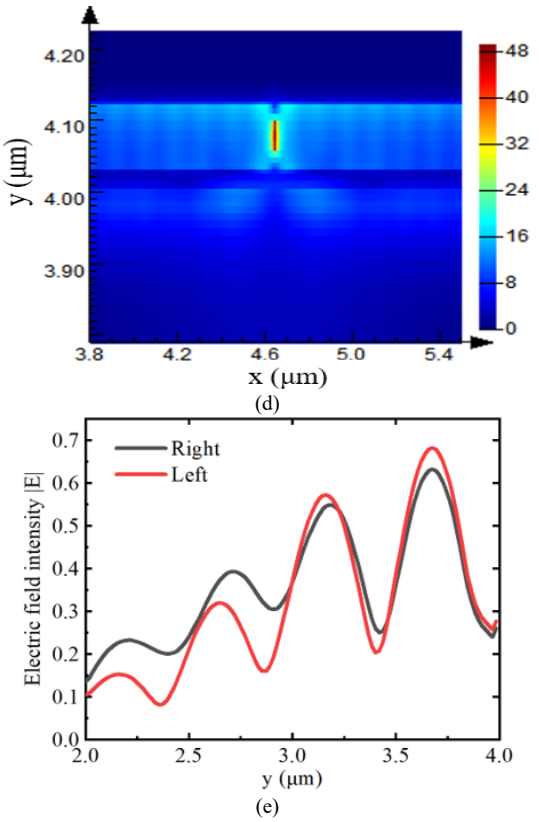

Fig.2 (a) The refractive index distribution of the simulation model in this work; (b) Simulated coupling efficiency under different Λ; (c) With Λ=310 nm, the local electric field intensity distribution of the simulation model; (d) The local electric field intensity distribution of the simulation model without the grating coupler; (e) The electric field intensity of the right and left light coupled into SU-8 waveguide core

(Microchem, SU-8 2002) was coated on glass substrate, which was soft baked at 65 ℃ for 10 min and 90 ℃ for 20 min. Then the sample was exposed by the interference of two beams with size of ~6 mm in diameter which were split from the UV laser (Spectra physics, LAB-150-10H). By changing the angle θ of beams, Λ can be adjusted according to the formula[27] $\Lambda=\lambda/2\sin\theta$, where λ is 355 nm of the laser. The exposure energy of the single laser beam was 0.85 mJ with exposure time of 1 s and the angle θ was set to 34.9° for the expected grating period Λ=310 nm. After the interference exposure, the UV light irradiation (ABM/6/350/NUV/DCCD/BSV/M) with a mask for 5 s was performed immediately to cure the unexposed SU-8 to form the waveguide. The UV opaque mask area with size of 2.5 mm×2.5 mm is located in the center of the interference pattern, which is larger than the light-emitting area of the OLED (2 mm×2 mm). Following the mask exposure, a post bake at 65 ℃ for 10 min and 90 ℃ for 20 min was done for SU-8 crosslinking[28]. When cooled down to room temperature, the sample was developed for 20 s to form the grating structure and a hard bake was done to evaporate developer. Next, the prepared SU-8 waveguide grat-

ing coupler was brought into a thermal evaporation chamber for subsequent deposition. A 20-nm-thick MoO_x was firstly deposited on the surface of the grating and the bottom-emission OLED with structure of Ag (18 nm)/Al (2 nm)/MoO_x (15 nm)/m-MTDATA (30 nm)/$Ir(ppy)_3$: TpBi (10 nm; 8wt%)/Bphen (40 nm)/LiF (1 nm)/Al (100 nm) was deposited sequentially at a base pressure of 5×10^{-4} Pa. All the materials were come from Luminescence Technology Corp. Fig.3(b) shows the measurement system which consists of a source meter unit (Keithley 2400) and an integrating sphere connected to the spectrometer (Ocean Optics, QEPro) through an optical fiber. The optical power, the current-density voltage (*J-V*) and spectra characteristics of the integrated devices were measured by this system in nitrogen glove box at dark environment.

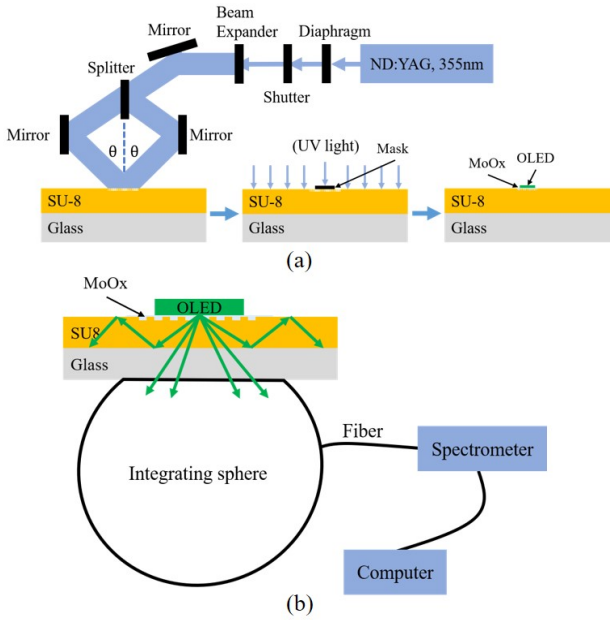

Fig.3 (a) The fabrication procedure of an OLED and SU-8 waveguide integrated device based on grating coupler; (b) The measurement schematic of the integrated device

To verify the grating parameters, the surface morphology of the fabricated grating was characterized by atomic force microscopy (Bruker Icon) in the tapping mode as shown in Fig.4(a). From Fig.4(a), the grating period and etch depth can be obtained about 330 nm and 15 nm, respectively. In order to investigate the effect of the grating coupler with 20 nm MoO_x buffer layer on the electrical properties of the OLED, the *J-V* characteristics of the OLEDs in the integrated devices of grating/OLED, grating/MoO_x/OLED and MoO_x/OLED were tested as shown in Fig.4(b). Compared with the device of grating/MoO_x/OLED, the *J-V* characteristics of the device grating/OLED have a decline. Under the same current-density condition, the higher the voltage, the worse the electrical properties. However, the *J-V* curves of the devices grating/MoO_x/OLED and MoO_x/OLED are approximately consistent, which indicates that the electrical properties of the OLED are not affected by the grating coupler with 20 nm MoO_x buffer layer. This may be due to the 20 nm MoO_x buffer layer can flatten the surface of the grating coupler.

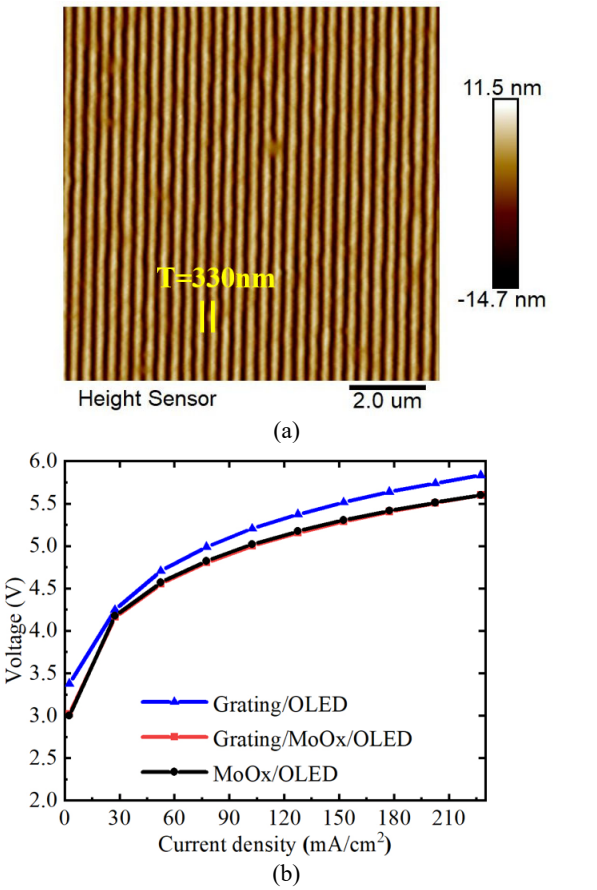

Fig.4 (a) The surface morphology of the grating characterized by atomic force microscopy; (b) The *J-V* curves of the OLEDs in the integrated devices

Fig.5(a) shows the electroluminescence (EL) spectra of the OLEDs in the integrated devices without and with grating coupler. It should be mentioned that the EL spectrums and the optical powers of the OLEDs were measured from the light transmitted from the glass substrate. The central wavelength of the OLED in the integrated device without grating coupler is 520 nm and shifts to 522 nm with grating coupler. Moreover, the EL intensity of the light near the central wavelength of the OLED has an obvious decrease. Since the OLEDs in the integrated devices without and with grating coupler have the nearly identical *J-V* characteristics, the decline of the EL intensity and the shift of the center wavelength are due to the grating coupler which could couple the light in specific wavelength range into the waveguide. Since a part of the light from the OLED through the grating coupler was coupled into SU-8 waveguide and the others were transmitted into the glass substrate, the transmitted optical power can be used to estimate the improved light coupling efficiency ($\Delta\eta$)[29] which could be expressed as

$$\Delta\eta=\frac{P_1-P_2}{P_1+P_1-P_2}, \quad (5)$$

where P_1 and P_2 are the transmitted optical power of the integrated devices without and with grating coupler, and P_1-P_2 can be considered as the increased optical power coupled into the waveguide due to the grating coupler.

Fig.5(b) shows the transmitted optical powers of the OLEDs in the integrated devices without and with grating coupler under different current densities. Owing to the fact that a part of the light is coupled into the waveguide, the transmitted optical powers of the integrated device with grating coupler have an obvious decrease under different current densities.

Fig.5(c) shows the improved coupling efficiencies under different current densities, which was calculated by Eq.(5).

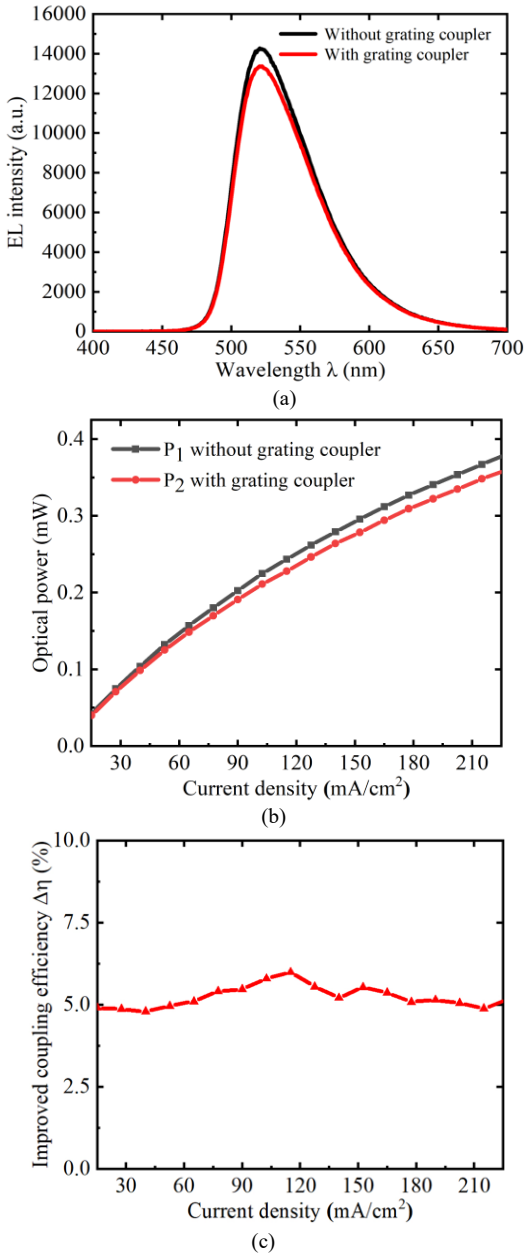

Fig.5 (a) The EL spectra of the OLEDs in the integrated devices without and with grating coupler; (b) The transmitted optical powers under different current densities; (c) The improved coupling efficiency $\Delta\eta$ under different current densities

According to Fig.5(c), $\Delta\eta$ is about 5%, which is smaller than the simulation result (6.65%) because the parameters of the fabricated grating coupler are a little different from the simulation results. Tab.1 shows how our work different from others.

Tab.1 Efficiencies of different coupling methods

Source	Waveguide	Method	η	Reference
OLED	PMMA	45° Au mirror	-	[12]
PLED	SU-8	SiO_2 particles	1%	[13]
PLED	Ta_2O_5	SiO_2 spacer	3.2%	[30]
OLED	SU-8	Grating coupler	5%	Our work

In summary, we have fabricated the integrated device of an OLED and polymer optical waveguide by introducing the grating coupler with an MoO_x buffer layer. Detailed investigations on the design of an OLED and polymer optical waveguide integrated device based on grating coupler with an MoO_x buffer layer have been presented. Experiments show that the grating coupler with an MoO_x buffer layer ensured the electrical properties of the integrated OLED without degradation. Meanwhile, we calculated the improved light coupling efficiency by comparing the transmitted optical powers of the integrated devices without and with grating coupler, which is in good agreement with the simulation result. It was proved that the grating coupler can effectively improve the light coupling efficiency of an OLED and polymer optical waveguide. Our work provides a simple and low-cost approach for monolithic integration of an OLED source and polymer optical waveguide which has the great potential in the field of optical sensing.

References

[1] G. Zhao, H. Dong, Q. Liao, J. Jiang, Y. Luo, H. Fu and W. Hu, Nature Communications **9**, 4790 (2018).

[2] Maik Rahlves, Axel Guenther, Maher Rezem and Bernhard Roth, Journal of Lightwave Technology **37**, 729 (2019).

[3] M. C. Estevez, M. Alvarez and L. M. Lechuga, Laser & Photonics Reviews **6**, 463 (2012).

[4] Adam L. Washburn and Ryan C. Bailey, Analyst **136**, 227 (2011).

[5] Vishak Venkatraman and Andrew J. Steckl, Biosensors & Bioelectronics **74**, 150 (2015).

[6] Y. Kim, S. Park, S. K. Park, S. Yun, K. U. Kyung and K. Sun, Optics Express **20**, 14486 (2012).

[7] M. Punke, S. Mozer, M. Stroisch, M. Gerken, G. Bastian, U. Lemmer, D. G. Rabus and P. Henzi, Organic Semiconductor Devices for Micro-Optical Applications,

Micro-Optics, Vcsels, and Photonic Interconnects II: Fabrication, Packaging, and Integration, Conference on Micro-Optics, VCSELs, and Photonic Interconnects II, 6185 (2006).

[8] C. Delezoide, M. Salsac, J. Lautru, H. Leh, C. Nogues, J. Zyss, M. Buckle, I. Ledoux-Rak and C. T. Nguyen, IEEE Photonics Technology Letters **24**, 270 (2012).

[9] B. Lamprecht, H. Ditibacher, G. Jakopic and J. R. Krenn, Physica Status Solidi-Rapid Research Letters **2**, 266 (2008).

[10] Jacob MV, Electronics **3**, 594 (2014).

[11] M. Diez, V. Raimbault, S. Joly, L. Oyhenart, J. B. Doucet, I. Obieta, C. Dejous and L. Bechou, Optical Materials **82**, 21 (2018).

[12] Y. Ohmori, H. Kajii, M. Kaneko, K. Yoshino, M. Ozaki, A. Fujii, M. Hikita, H. Takenaka and T. Taneda, IEEE Journal of Selected Topics in Quantum Electronics **10**, 70 (2004).

[13] Yuan-Yu Lin, Chung Cheng, Hua-Hsien Liao, Sheng-Fu Horng, Hsin-Fei Meng and Chain-Shu Hsu, Applied Physics Letters **89**, 379 (2006).

[14] Daphne Duval, Ana Belen Gonzalez-Guerrero, Stefania Dante, Johann Osmond, Rosa Monge, Luis J. Fernandez, Kirill E. Zinoviev, Carlos Dominguez and Laura M. Lechuga, Lab on a Chip **12**, 1987 (2012).

[15] T. Pustelny and P. Struk, Opto-Electronics Review **20**, 201 (2012).

[16] J. Sakamoto, T. Hashimoto, H. Kawata and Y. Hirai, Journal of Photopolymer Science and Technology **32**, 15 (2019).

[17] Y. Xin, G. Pandraud, Y. M. Zhang and P. French, Sensors **19**, 12 (2019).

[18] Christoph Prokop, Steffen Schoenhardt, Bert Laegel, Sandra Wolff, Arnan Mitchell and Christian Karnutsch, Journal of Lightwave Technology **34**, 3966 (2016).

[19] R. Singh, R. R. Singh and V. Priye, Optical and Quantum Electronics **51**, 10 (2019).

[20] Pei Li, Alex Dorn, Maher Rezem, Kirsten Honnef and Hans Zappe, Applied Optics **57**, 5161 (2018).

[21] Sanjeev Kumar Raghuwanshi, Indian Journal of Physics **84**, 831 (2010).

[22] U. Akin and H. Safak, Journal of Alloys and Compounds **647**, 146 (2015).

[23] D. Taillaert, F. Van Laere, M. Ayre, W. Bogaerts, D. VanThourhout, P. Bienstman and R. Baets, Japanese Journal of Applied Physics Part 1-Regular Papers Brief Communications & Review Papers **45**, 6071 (2006).

[24] C. Zhang, J. H. Sun, X. Xiao, W. M. Sun, X. J. Zhang, T. Chu, J. Z. Yu and Y. D. Yu, Chinese Physics Letters **30**, 4 (2013).

[25] M. H. Lu and J. C. Sturm, Journal of Applied Physics **91**, 595 (2002).

[26] C. Y. Huang, X. P. Zhang, J. S. Wang and C. Y. Hong, Advanced Optical Materials **6**, 9 (2018).

[27] J. Skriniarova, D. Pudis, I. Martincek, J. Kovac, N. Tarjanyi, M. Vesely and I. Turek, Microelectronics Journal **38**, 746 (2007).

[28] K. Venkatakrishnan, S. Jariwala and B. Tan, Optics Express **17**, 2756 (2009).

[29] Y. Dong, Y. M. Sun, Y. F. Li, X. Q. Yu, X. Y. Hou and X. Zhang, Thin Solid Films **516**, 1214 (2008).

[30] Marc Ramuz, Lukas Buergi, Ross Stanley and Carsten Winnewisser, Journal of Applied Physics **105**, 4652 (2009).